

**NATIONAL ADVISORY COMMITTEE  
FOR AERONAUTICS**

---

**REPORT No. 566**

**GROUND-HANDLING FORCES ON A 1/40-SCALE  
MODEL OF THE U. S. AIRSHIP "AKRON"**

By **ABE SILVERSTEIN** and **B. G. GULICK**



**1936**

## AERONAUTIC SYMBOLS

### 1. FUNDAMENTAL AND DERIVED UNITS

	Symbol	Metric		English	
		Unit	Abbrevia- tion	Unit	Abbrevia- tion
Length.....	<i>l</i>	meter.....	m	foot (or mile).....	ft. (or mi.)
Time.....	<i>t</i>	second.....	s	second (or hour).....	sec. (or hr.)
Force.....	<i>F</i>	weight of 1 kilogram.....	kg	weight of 1 pound.....	lb.
Power.....	<i>P</i>	horsepower (metric).....		horsepower.....	hp.
Speed.....	<i>V</i>	{kilometers per hour..... meters per second.....	{k.p.h. m.p.s.	{miles per hour..... feet per second.....	{m.p.h. f.p.s.

### 2. GENERAL SYMBOLS

<p><i>W</i>, Weight = <math>mg</math></p> <p><i>g</i>, Standard acceleration of gravity = 9.80665 m/s<sup>2</sup> or 32.1740 ft./sec.<sup>2</sup></p> <p><i>m</i>, Mass = <math>\frac{W}{g}</math></p> <p><i>I</i>, Moment of inertia = <math>mk^2</math>. (Indicate axis of radius of gyration <i>k</i> by proper subscript.)</p> <p><i>μ</i>, Coefficient of viscosity</p>	<p><i>ν</i>, Kinematic viscosity</p> <p><i>ρ</i>, Density (mass per unit volume) Standard density of dry air, 0.12497 kg-m<sup>-4</sup>-s<sup>2</sup> at 15° C. and 760 mm; or 0.002378 lb.-ft.<sup>-4</sup> sec.<sup>2</sup> Specific weight of "standard" air, 1.2255 kg/m<sup>3</sup> or 0.07651 lb./cu.ft.</p>
--	--

### 3. AERODYNAMIC SYMBOLS

<p><i>S</i>, Area</p> <p><i>S<sub>w</sub></i>, Area of wing</p> <p><i>G</i>, Gap</p> <p><i>b</i>, Span</p> <p><i>c</i>, Chord</p> <p><math>\frac{b^2}{S}</math>, Aspect ratio</p> <p><i>V</i>, True air speed</p> <p><i>q</i>, Dynamic pressure = <math>\frac{1}{2}\rho V^2</math></p> <p><i>L</i>, Lift, absolute coefficient <math>C_L = \frac{L}{qS}</math></p> <p><i>D</i>, Drag, absolute coefficient <math>C_D = \frac{D}{qS}</math></p> <p><i>D<sub>o</sub></i>, Profile drag, absolute coefficient <math>C_{D_o} = \frac{D_o}{qS}</math></p> <p><i>D<sub>i</sub></i>, Induced drag, absolute coefficient <math>C_{D_i} = \frac{D_i}{qS}</math></p> <p><i>D<sub>p</sub></i>, Parasite drag, absolute coefficient <math>C_{D_p} = \frac{D_p}{qS}</math></p> <p><i>C</i>, Cross-wind force, absolute coefficient <math>C_C = \frac{C}{qS}</math></p> <p><i>R</i>, Resultant force</p>	<p><i>i<sub>w</sub></i>, Angle of setting of wings (relative to thrust line)</p> <p><i>i<sub>t</sub></i>, Angle of stabilizer setting (relative to thrust line)</p> <p><i>Q</i>, Resultant moment</p> <p><i>Ω</i>, Resultant angular velocity</p> <p><math>\frac{\rho V l}{\mu}</math>, Reynolds Number, where <i>l</i> is a linear dimension (e.g., for a model airfoil 3 in. chord, 100 m.p.h. normal pressure at 15° C., the corresponding number is 234,000; or for a model of 10 cm chord, 40 m.p.s. the corresponding number is 274,000)</p> <p><i>C<sub>p</sub></i>, Center-of-pressure coefficient (ratio of distance of <i>c.p.</i> from leading edge to chord length)</p> <p><i>α</i>, Angle of attack</p> <p><i>ε</i>, Angle of downwash</p> <p><i>α<sub>o</sub></i>, Angle of attack, infinite aspect ratio</p> <p><i>α<sub>i</sub></i>, Angle of attack, induced</p> <p><i>α<sub>a</sub></i>, Angle of attack, absolute (measured from zero-lift position)</p> <p><i>γ</i>, Flight-path angle</p>
--	--

---

---

**REPORT No. 566**

---

**GROUND-HANDLING FORCES ON A 1/40-SCALE  
MODEL OF THE U. S. AIRSHIP "AKRON"**

**By ABE SILVERSTEIN and B. G. GULICK**  
**Langley Memorial Aeronautical Laboratory**

## NATIONAL ADVISORY COMMITTEE FOR AERONAUTICS

HEADQUARTERS, NAVY BUILDING, WASHINGTON, D. C.

LABORATORIES, LANGLEY FIELD, VA.

Created by act of Congress approved March 3, 1915, for the supervision and direction of the scientific study of the problems of flight (U. S. Code, Title 50, Sec. 151). Its membership was increased to 15 by act approved March 2, 1929. The members are appointed by the President, and serve as such without compensation.

JOSEPH S. AMES, Ph. D., *Chairman*,  
Baltimore, Md.

DAVID W. TAYLOR, D. Eng., *Vice Chairman*,  
Washington, D. C.

CHARLES G. ABBOT, Sc. D.,  
Secretary, Smithsonian Institution.

LYMAN J. BRIGGS, Ph. D.,  
Director, National Bureau of Standards.

ARTHUR B. COOK, Rear Admiral, United States Navy,  
Chief, Bureau of Aeronautics, Navy Department.

WILLIS RAY GREGG, B. A.,  
United States Weather Bureau.

HARRY F. GUGGENHEIM, M. A.,  
Port Washington, Long Island, N. Y.

SYDNEY M. KRAUS, Captain, United States Navy,  
Bureau of Aeronautics, Navy Department.

CHARLES A. LINDBERGH, LL. D.,  
New York City.

WILLIAM P. MACCRACKEN, Jr., LL. D.,  
Washington, D. C.

AUGUSTINE W. ROBINS, Brigadier General, United States Army,  
Chief Matériel Division, Air Corps, Wright Field, Dayton,  
Ohio.

EUGENE L. VIDAL, C. E.,  
Director of Air Commerce, Department of Commerce.

EDWARD P. WARNER, M. S.,  
New York City.

OSCAR WESTOVER, Major General, United States Army,  
Chief of Air Corps, War Department.

ORVILLE WRIGHT, Sc. D.,  
Dayton, Ohio.

---

GEORGE W. LEWIS, *Director of Aeronautical Research*

JOHN F. VICTORY, *Secretary*

HENRY J. E. REID, *Engineer in Charge, Langley Memorial Aeronautical Laboratory, Langley Field, Va.*

JOHN J. IDE, *Technical Assistant in Europe, Paris, France*

---

### TECHNICAL COMMITTEES

AERODYNAMICS

POWER PLANTS FOR AIRCRAFT

AIRCRAFT STRUCTURES AND MATERIALS

AIRCRAFT ACCIDENTS

INVENTIONS AND DESIGNS

*Coordination of Research Needs of Military and Civil Aviation*

*Preparation of Research Programs*

*Allocation of Problems*

*Prevention of Duplication*

*Consideration of Inventions*

LANGLEY MEMORIAL AERONAUTICAL LABORATORY

LANGLEY FIELD, VA.

Unified conduct, for all agencies, of scientific research on the fundamental problems of flight.

OFFICE OF AERONAUTICAL INTELLIGENCE

WASHINGTON, D. C.

Collection, classification, compilation, and dissemination of scientific and technical information on aeronautics.

## REPORT No. 566

### GROUND-HANDLING FORCES ON A 1/40-SCALE MODEL OF THE U. S. AIRSHIP "AKRON"

By ABE SILVERSTEIN and B. G. GULICK

#### SUMMARY

An investigation was conducted in the N. A. C. A. full-scale wind tunnel to determine the ground-handling forces on a 1/40-scale model of the U. S. airship "Akron." Ground-handling conditions were simulated by establishing a velocity gradient above a special ground board in the tunnel comparable with that encountered over a landing field. The tests were conducted at Reynolds Numbers ranging from 5,000,000 to 19,000,000 at each of six angles of yaw between 0° and 180° and at four heights of the model above the ground board.

The ground-handling forces vary greatly with the angle of yaw and reach large values at appreciable angles of yaw. Small changes in height, pitch, or roll did not critically affect the forces on the model. In the range of Reynolds Numbers tested, no significant variation of the forces with the scale was disclosed.

#### INTRODUCTION

At the request of the Bureau of Aeronautics, Navy Department, an investigation was conducted in the N. A. C. A. full-scale wind tunnel to determine the ground-handling forces on a 1/40-scale model of the U. S. airship *Akron*.

Correlated data on the forces and moments encountered in handling airships near the ground have not been available. Previous work of a similar nature conducted at low Reynolds Numbers has shown conflicting results (references 1 and 2). Actual handling experiences with the large airships have shown under some conditions the existence of extremely large forces and moments that may endanger the airship unless properly anticipated. The prediction of the numerical values of the handling forces by wind-tunnel research is not satisfactory owing to the relatively small size of the models. It was believed, however, that the 1/40-scale *Akron* model was large enough to enable the direction and trend of the forces to be predicted.

Ground-handling conditions were closely simulated by establishing a velocity gradient above the ground board comparable with that encountered over a landing field. Tests were made at six angles of yaw between 0° and 180°, at four heights of the model above the

ground board, and at air speeds from 28 to 100 miles per hour. Several special conditions of pitch and roll were also investigated.

#### WIND TUNNEL AND EQUIPMENT

The wind tunnel used for these tests is described in reference 3. The tunnel was modified by the addition of a horizontal ground board, 30 feet wide, to simulate the landing field. The board was installed at the level of the lower surface of the entrance cone, making a continuous surface with the entrance cone and extend-

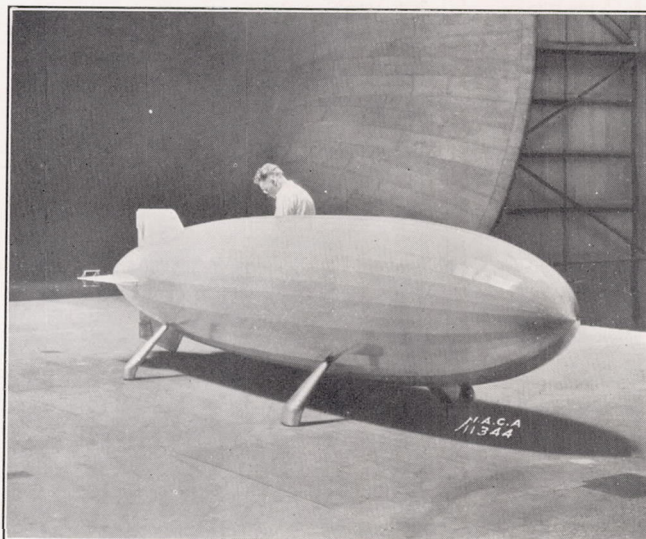


FIGURE 1.—The 1/40-scale model of the U. S. airship *Akron* on ground board at 0° yaw.

ing to within a few feet of the exit cone. Figure 1 shows the model in position above the ground board.

Forces, moments, and velocity distribution about the model were measured with the standard wind-tunnel equipment. The model was supported by four struts projecting through the ground board and rigidly attached at their lower ends to the floating frame of the balance (fig. 1). The portions of the struts extending above the ground board were shielded by streamline fairings to eliminate tare forces.

Smoke was used to show the flow of air over the model. The smoke was generated by passing kerosene

through heated coils and was ejected through small tubes into the air stream a short distance ahead of the model. Pictures were taken of the flow with a standard movie camera using 16 millimeter film and taking 16 frames a second.

### MODEL

The *Akron* model previously tested in the propeller-research tunnel (reference 4) was fitted with the Mark II fins and control surfaces. The model is of hollow wood construction of polygonal cross section with 36 sides over the fore part of the hull faired into 24 sides near the stern. The surface was refinished so as to be comparable with well-doped fabric. The principal dimensions of the model are listed in the following table:

Ratio of distance from nose to total length	Radius (circumscribed circle)
$a/L$	Inches
0	0
.02	4.95
.05	9.96
.10	14.20
.15	16.65
.20	18.39
.25	19.12
.30	19.61
.35	19.85
.40	19.90
.45	19.90
.50	19.80
.55	19.59
.60	19.12
.65	18.46
.70	17.50
.75	16.15
.80	14.44
.85	12.29
.90	9.61
.95	6.52
1.00	0

Length, 19.62 ft.; volume, 115 cu. ft.;  $(\text{vol})^{2/3}$ , 23.62 sq. ft.;  $(\text{vol})^{1/3}$ , 4.86 ft.; center of buoyancy,  $a/L=0.464$ .

### VELOCITY GRADIENT

One of the important variables affecting the airship handling forces is the gradient of the wind velocity with height above the landing field. This velocity gradient is not constant and depends largely on the terrain and the weather conditions. In the present investigation it

was not expedient to test with more than one velocity gradient so that a representative gradient obtained in tests at Langley Field (reference 5) was adopted. This reference velocity gradient indicates that the average increase in velocity with height above the ground is proportional to the 1/7 power of the height ( $V \propto h^{1/7}$ ) or, in terms of the dynamic pressure,  $q \propto h^{2/7}$ . This velocity gradient is similar to that in the boundary layer of a flat plate immersed in a turbulent stream at high Reynolds Numbers and may be considered as the most probable gradient over a flat landing field free of obstructions.

The velocity at 200 feet above the ground was arbitrarily chosen as a reference. It corresponds to a height of 5 feet above the ground board for the model tests; consequently all velocity computations are based on the velocity at this height. The gradients as represented by the foregoing relation and as determined from the results of dynamic-pressure surveys for the positions occupied by the model are compared in figure 2.

### CORRECTIONS

The results were corrected for the blocking effect of the model on the air stream. (See reference 6.) Inasmuch as the model was small in proportion to the size of the jet, no tunnel-boundary corrections were applied to the data. Surveys showed the variation of the static pressure over the length of the model to be negligible, therefore no corrections for static-pressure gradient were made.

### TESTS

**Force tests.**—The lift, drag, and cross-wind forces and the pitching, rolling, and yawing moments were measured for four heights, 25½, 27, 28½, and 31½ inches, of the model center line above the ground board (fig. 3). These heights gave clearances between the ground board and the model at the maximum diameter of 5.6, 7.1, 8.6, and 11.6 inches, respectively. Tests were made at each height for the following six angles of yaw relative to the wind: 0°, 30°, 60°, 90°, 180°, and

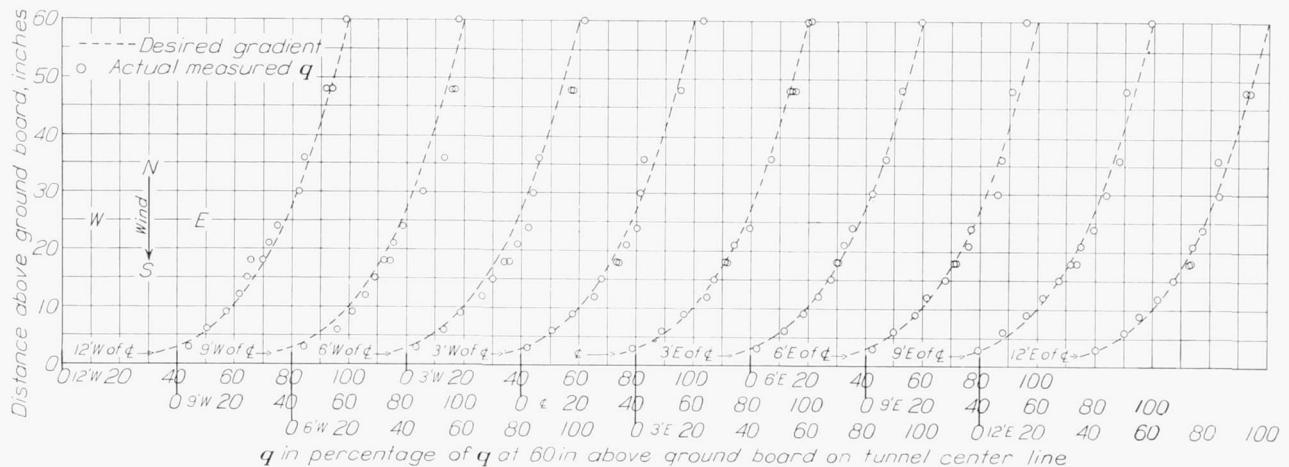


FIGURE 2.—Velocity gradient for ground-handling tests of the 1/40-scale model of the U. S. airship *Akron*.

210°. The angle of yaw of 210° instead of 150° was used for convenience in testing. The magnitudes of the forces and moments are obviously the same for the two angles but the direction is opposite for the cross-wind force and the rolling and yawing moments. For the comparison of the results, the coefficients for 210° yaw angle were converted to 150° yaw.

At the 28½-inch height, tests were made with the model rolled to the right through an angle of 10° while yawed at angles of 30° and 90°. The effects of small angles of pitch were obtained by pitching the model 2° and -2° (fig. 3); the forces and moments were measured for the 0°, 30°, and 180° yaw positions.

For the tests with the model in roll, the Reynolds Numbers ranged from 5,000,000 to 8,000,000. All other tests were made at Reynolds Numbers ranging from 5,000,000 to 19,000,000, which correspond to air speeds from 28 to 100 miles per hour. The Reynolds Number values are based on the length of the hull,

$$\text{Reynolds Number} = \frac{\rho V l}{\mu}$$

and are 4.04 times those based on  $(\text{vol})^{1/3}$ , which have been used in a number of airship investigations.

**Smoke flow.**—Motion pictures were taken of smoke flow over several sections along the model for all angles of yaw with the model 28½ inches above the ground board. Enlarged prints (fig. 4) illustrate the nature of the flow.

**Wake surveys.**—Surveys were made of the dynamic pressure and total head in the field of the model when yawed 90° to the wind.

## RESULTS

The results of the force tests are presented (figs. 5 to 24) in the form of nondimensional coefficients defined as follows:

Lift coefficient,

$$C_L = \frac{\text{lift}}{q(\text{vol})^{2/3}}$$

Drag coefficient,

$$C_D = \frac{\text{drag parallel to wind axes}}{q(\text{vol})^{2/3}}$$

Longitudinal-force coefficient,

$$C_X = \frac{\text{force parallel to longitudinal body axes}}{q(\text{vol})^{2/3}}$$

Cross-wind force coefficient,

$$C_{SS} = \frac{\text{cross-wind force}}{q(\text{vol})^{2/3}}$$

Cross-force coefficient,

$$C_Y = \frac{\text{force normal to longitudinal body axes}}{q(\text{vol})^{2/3}}$$

Resultant-force coefficient,

$$C_R = \frac{\text{resultant force}}{q(\text{vol})^{2/3}}$$

Rolling-moment coefficient,

$$C_l = \frac{\text{rolling moment about C. B.}}{q(\text{vol})}$$

Pitching-moment coefficient,

$$C_m = \frac{\text{pitching moment about C. B.}}{q(\text{vol})}$$

Yawing-moment coefficient,

$$C_n = \frac{\text{yawing moment about C. B.}}{q(\text{vol})}$$

in which (vol) is the volume of the hull in cubic feet and  $q$  is the dynamic pressure in pounds per square foot at a point 5 feet above the ground board, which corresponds to 200 feet above the ground for the full-size airship. When applying the wind-tunnel results to the actual airship, the wind velocity at a point 200 feet above the ground should be used as a base. All moment coefficients are presented with reference to the body axes of the model.

The important results are presented in their simplest form in figure 5, a three-view drawing of the measured

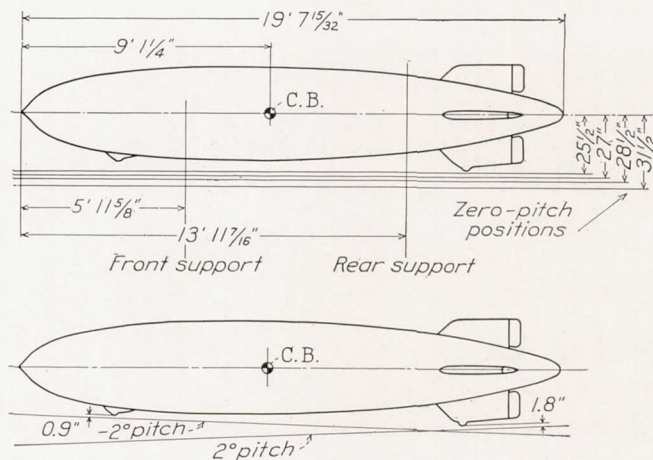
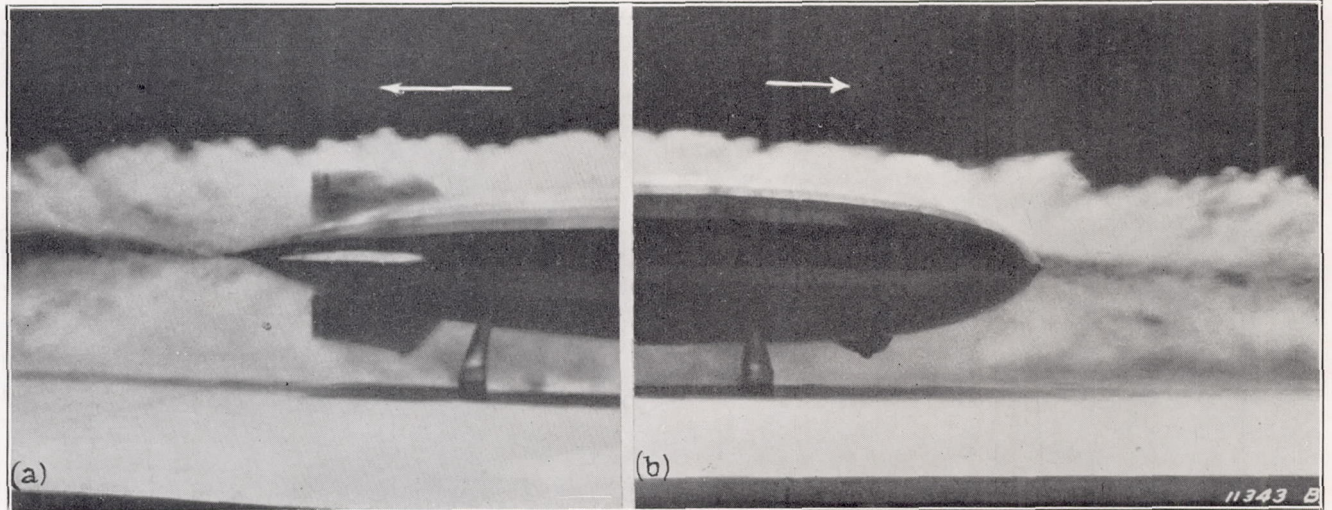


FIGURE 3.—Positions of the airship model relative to the ground board.

resultant-force vectors on the airship for the angles of yaw that were tested for a single height of the model above the ground. The vectors are to scale and show the magnitude and direction of the forces and the moments about the three coordinate axes.

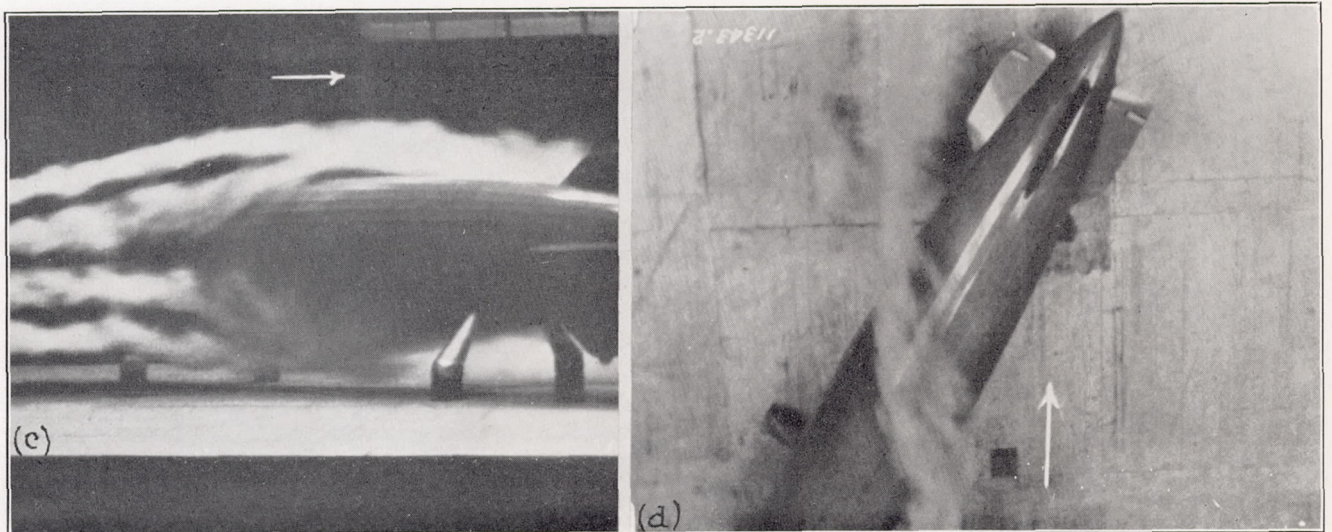
**Lift.**—The measured vertical forces on the airship model were positive, or upward, for the entire range of angles of yaw tested and for all heights of the model above the ground plane (fig. 6). The lift coefficient is negligible at 0° angle of yaw but increases with angle of yaw and reaches a maximum at an angle of about 60° to the relative wind. With increasing angles of yaw from 60° the lift decreases rapidly until at 90° it has a small positive value. In the angle range between 90° and 180° the lift decreases slowly and almost uniformly and becomes negligible again at 180° yaw.

In the scale range investigated the lift showed only a small variation with Reynolds Number for the 0° angle position but, at the 90° yaw angle, decreased at a small but constant rate with increasing Reynolds Number (figs. 7 and 8). The lift varies appreciably with the height of the model above the ground plane;



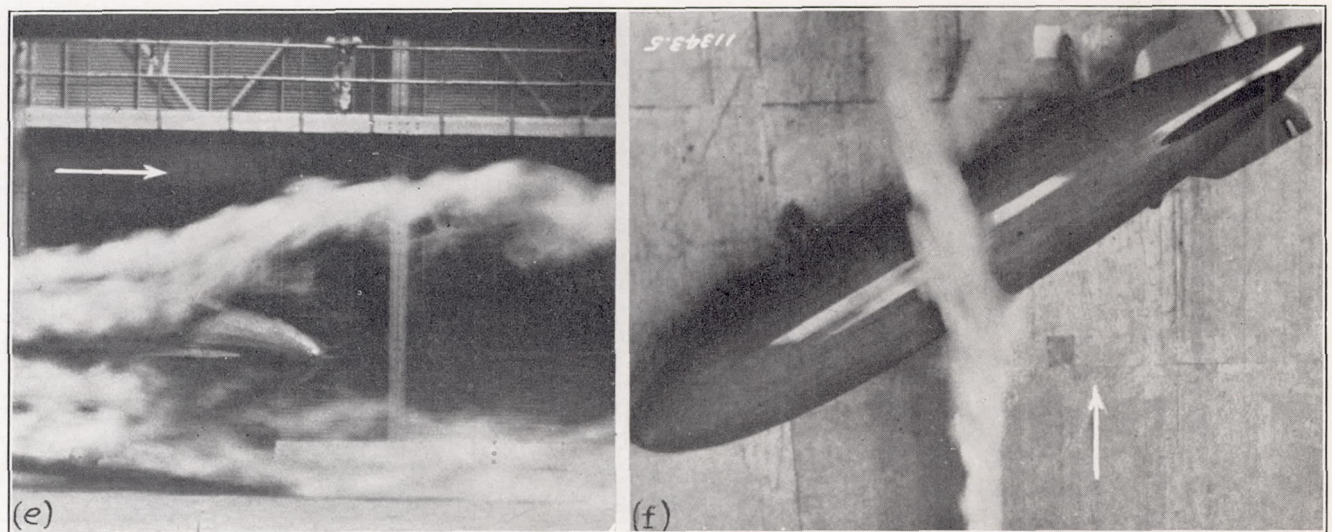
(a) Flow over tail at 0° yaw.

(b) Flow over nose at 180° yaw.



(c) Flow over midsection at 30° yaw, side view.

(d) Flow over midsection at 30° yaw, top view.

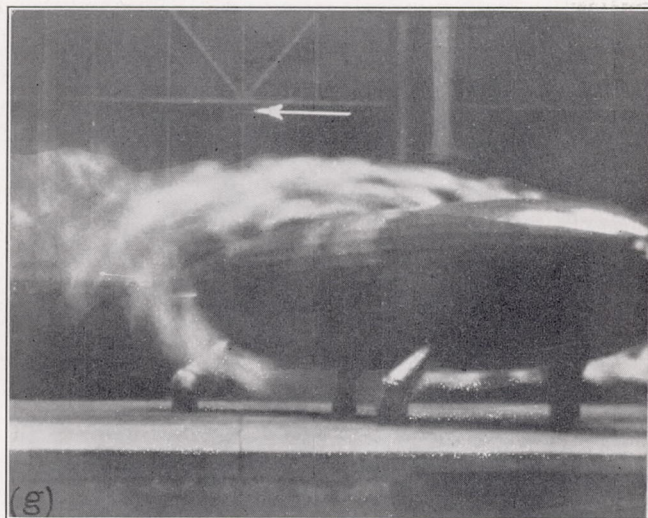


(e) Flow over tail at 30° yaw.

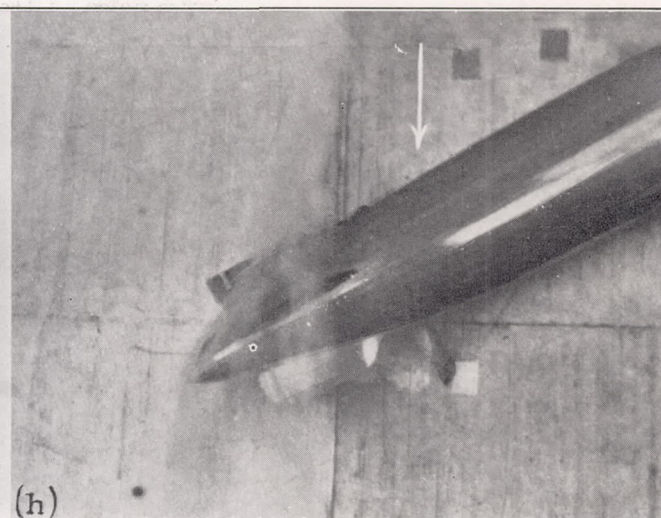
(f) Flow over midsection at 60° yaw.

FIGURE 4.—Smoke flow over 1/40-scale model of the U. S. airship *Akron*. Center line of model 28½ inches above the ground board.

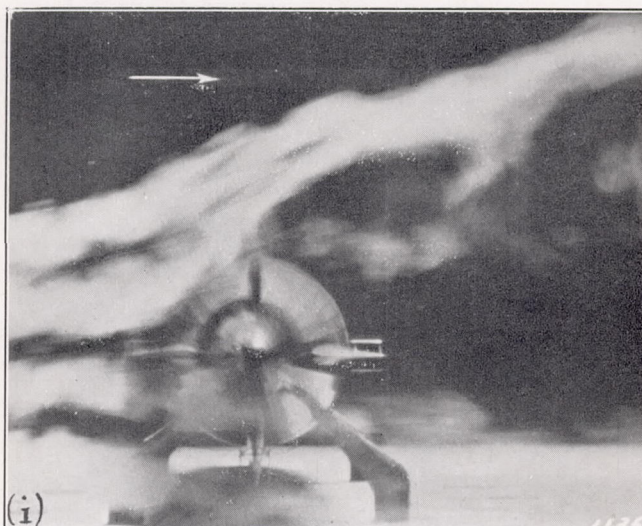




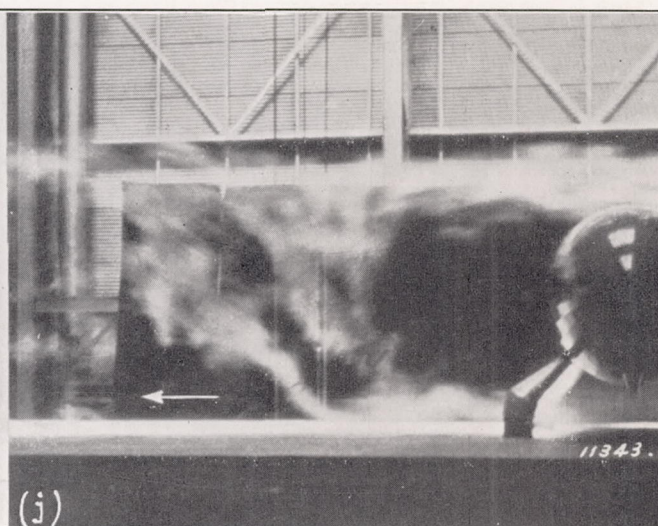
(g) Flow over midsection at 60° yaw.



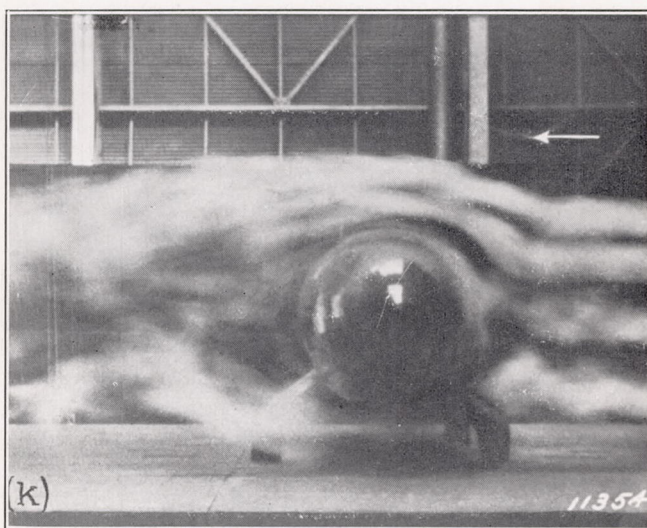
(h) Flow over tail at 60° yaw.



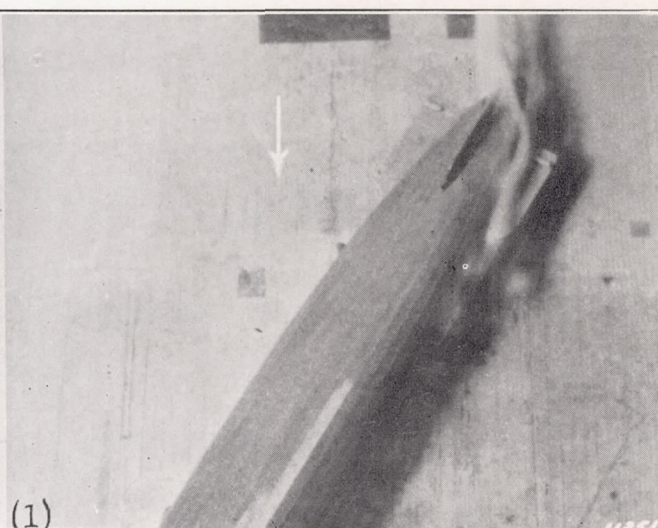
(i) Flow over tail at 90° yaw.



(j) Flow over midsection at 90° yaw.



(k) Flow over nose at 90° yaw.



(l) Flow over tail at 210° yaw.

FIGURE 4.—Continued. Smoke flow over 1/40-scale model of the U. S. airship *Akron*. Center line of model 28½ inches above the ground board.

however, the results showed that there were no critical heights in the range investigated. The lift on the model increases as the ground board is approached (fig. 6), showing the greatest absolute increase at about 60° yaw at which angle the lift is highest, but showing the greatest percentage increase in the angle range between 90° and 180°. Rolling the airship 10° made no appreciable change in the lift (fig. 9).

and is relatively unaffected by any of the changes in model height or roll (fig. 12).

The effect of scale on the longitudinal force is relatively unimportant in the Reynolds Number range tested as is shown in figures 7 and 8 for the 0° and 90° angles, respectively.

**Cross-wind force.**—Like the drag, the cross-wind force showed very little change with any of the varia-

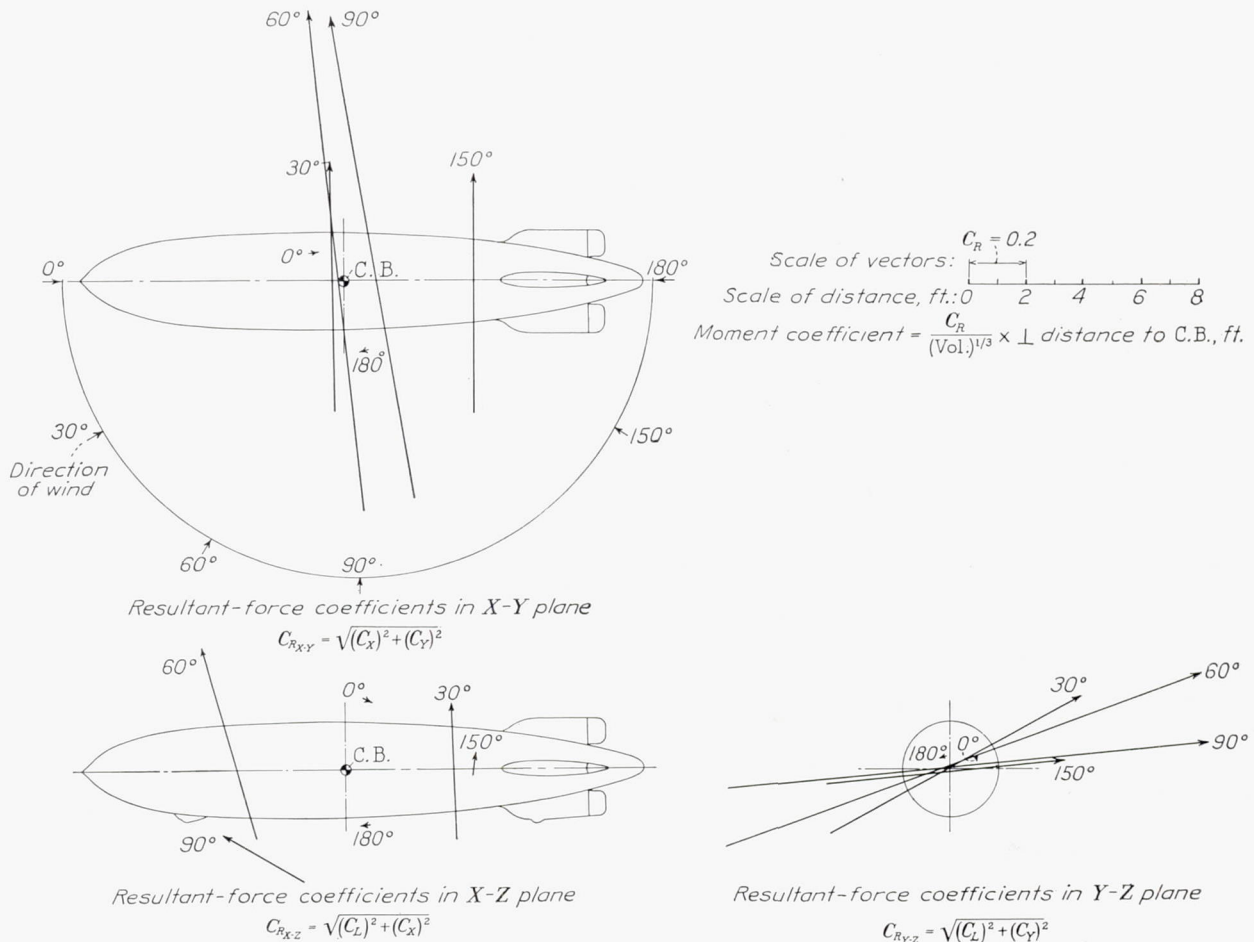


FIGURE 5.—Three-view drawing showing resultant forces on the 1/40-scale model of the U. S. airship *Akron*. Model 28½ inches above ground board. Reynolds Number, 16,000,000.

**Drag.**—The drag coefficients with reference to the wind axis increase as the angle of yaw increases and reach a maximum with the airship at 90° yaw. The drag curve is almost symmetrical about the 90° ordinate, and the drag coefficient drops to a value of about 0.030 for both the 0° and 180° angles (fig. 10). The height of the model above the ground plane proved to be an unimportant variable in the drag except in the range of angles near 90°. At the 90° angle the drag is lower for positions closer to the board.

The longitudinal-force coefficient (figs. 11 and 12) changes from a small positive value at 0° to a rather large negative or stern-to-bow force at 90°, the transition from positive to negative force occurring at about 30° yaw. The curve is essentially symmetrical

in model height, pitch, or roll (figs. 13, 14, and 15). In the range of angles near 90° yaw (fig. 14) the cross force (body axis) changes with model height, increasing with the greater distance from the board.

The cross force showed a greater variation with the Reynolds Number than did the longitudinal force, dropping off at the lower values to about 8 percent below the value for the high Reynolds Numbers (fig. 8).

**Pitching moment.**—The pitching moment was not critically affected by any of the variations in model height, pitch, or roll, and the results (figs. 16 and 17) again show that the effects of these variables were relatively unimportant compared with the changes in the pitching moment for small changes in the angle of yaw.

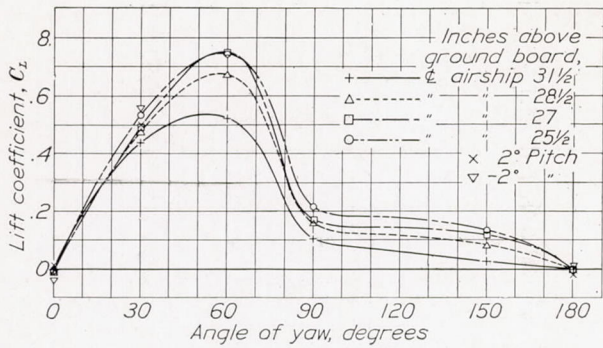


FIGURE 6.—The variation of the lift coefficient with angle of yaw, angle of pitch, and height above the ground board at a Reynolds Number of 16,000,000.

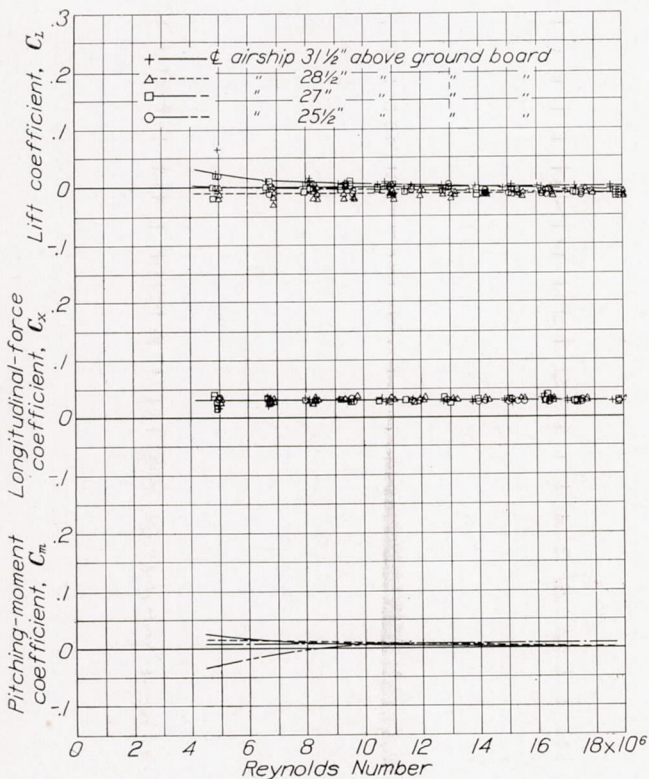


FIGURE 7.—The variation of the pitching-moment coefficient, the longitudinal-force coefficient, and the lift coefficient with Reynolds Number. Model at 0° yaw.

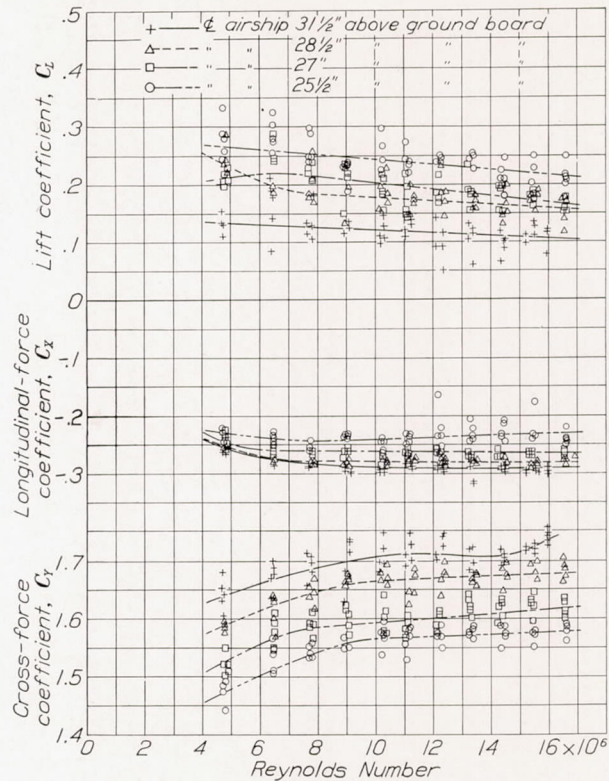


FIGURE 8.—The variation of the cross-force coefficient, the longitudinal-force coefficient, and the lift coefficient with Reynolds Number. Model at 90° yaw.

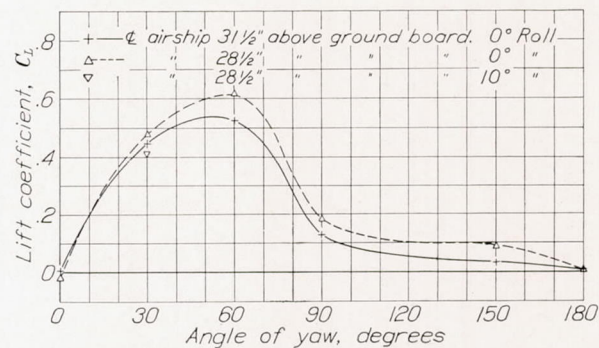


FIGURE 9.—The variation of the lift coefficient with angle of yaw, angle of roll, and height above the ground board at a Reynolds Number of 8,000,000.

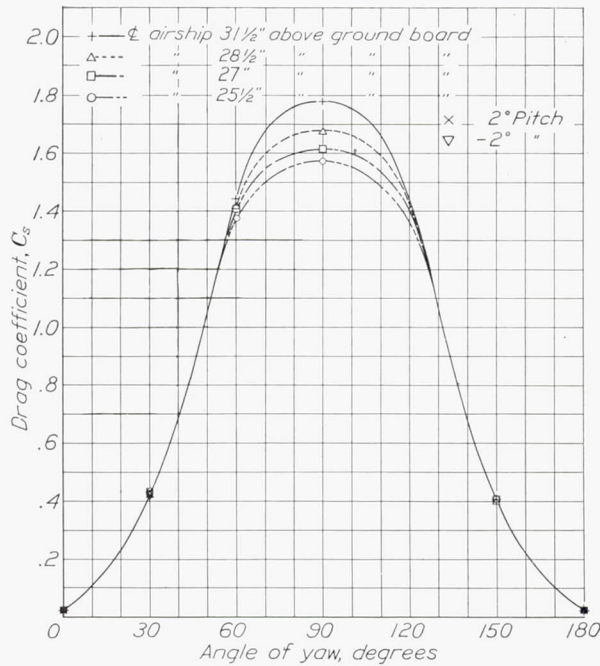


FIGURE 10.—The variation of the drag coefficient with angle of yaw, angle of pitch, and height above the ground board at a Reynolds Number of 16,000,000.

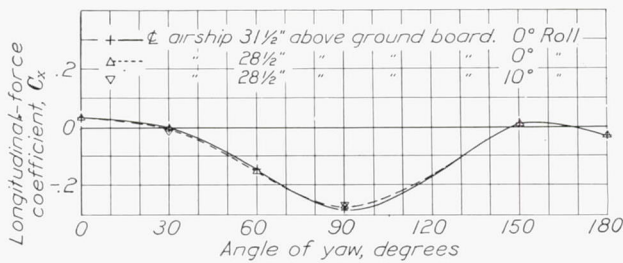


FIGURE 12.—The variation of longitudinal-force coefficient with angle of yaw, angle of roll, and height above the ground board at a Reynolds Number of 8,000,000.

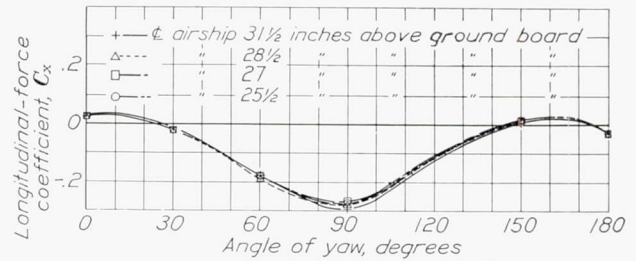


FIGURE 11.—The variation of the longitudinal-force coefficient with angle of yaw and height above the ground board at a Reynolds Number of 16,000,000.

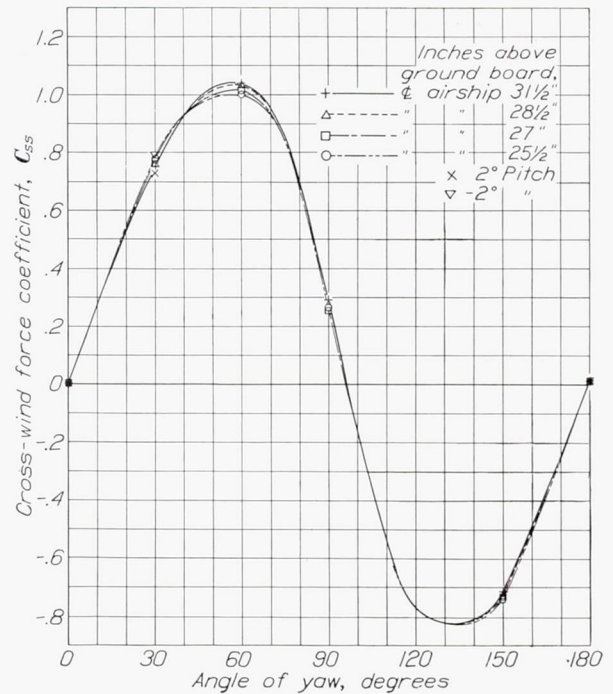


FIGURE 13.—The variation of cross-wind force with angle of yaw, angle of pitch, and height above the ground board at a Reynolds Number of 16,000,000.

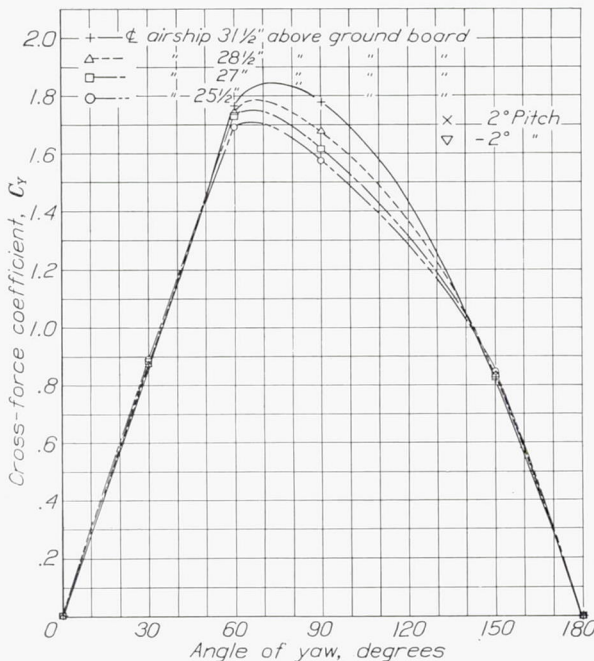


FIGURE 14.—The variation of cross-force coefficient with angle of yaw, angle of pitch, and height above the ground board at a Reynolds Number of 16,000,000.

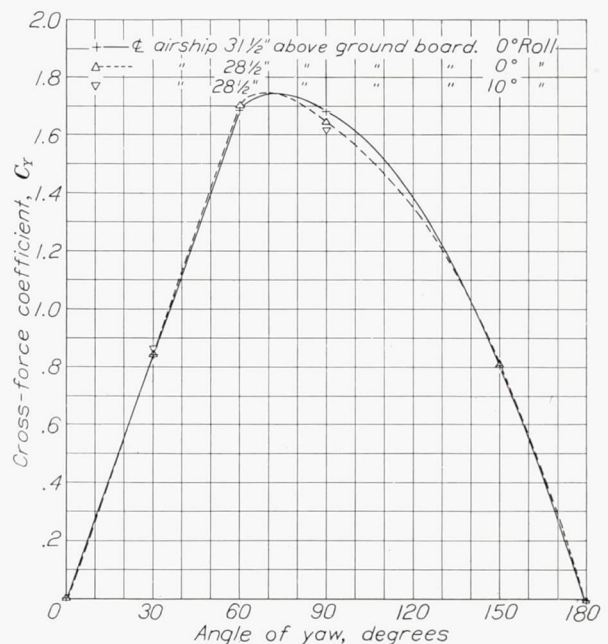


FIGURE 15.—The variation of cross-force coefficient with angle of yaw, angle of roll, and height above the ground board at a Reynolds Number of 8,000,000.

The variations of the pitching moment with the Reynolds Number were small and inconsistent as shown by figures 7 and 18 for the 0° and 90° yaw positions, respectively.

An interesting reversal of the sign of the pitching moment occurs in the yaw-angle range between 30° and 60°, the pitching-moment coefficient changing from about -0.35 at 30° to 0.55 at 60°.

**Yawing moment.**—The yawing-moment coefficients for angles of yaw in the range between 0° and 60° are small but reach large negative values at 150° (figs. 19 and 20). The effects of model height are unimportant except in the angle range between 0° and 60°, where the moments are small. The effects of roll and pitch are also relatively unimportant. The variation with Reynolds Number is small (fig. 18).

**Rolling moment.**—The rolling-moment coefficients are almost zero for the full range of the tests, and none of the variations in model height, pitch, roll, or Reynolds Number showed any marked or appreciable effects (figs. 18, 21, and 22).

**Wake surveys.**—The dynamic and total pressures in the wake of the airship at 90° yaw are presented in figures 23 and 24, respectively. The dead-wake size varies with position along the hull and is largest behind the tail surfaces.

#### DISCUSSION

The test results presented in figures 5 to 24 give directly the measured forces and moments on the 1/40-scale airship model for the conditions that were tested. It is desirable that some understanding be obtained of the origin of these forces and the nature of the flow about the airship to aid in the large extrapolation of the measured results to full-scale Reynolds Numbers. An attempt has therefore been made in the following paragraphs to analyze the test data and the general problem with a view to determining the nature of the flow about the airship when adjacent to the ground and to obtain some conception of the applicability of the results to the full-size airship. These fundamental conceptions are usually provided by the theory; however, the complex interaction of the effects of the ground gradient with those of the ground-plane interference makes any theoretical treatment without innumerable assumptions very difficult, if not impossible. The motion pictures taken of the smoke flow over the model, a few frames of which are presented in figure 4, greatly assisted in the flow analysis.

The following problems are considered to be of particular interest and importance and will be discussed in the succeeding paragraphs:

1. The source of the positive lifting force on the model.
2. Possibilities of extrapolating the lift results to Reynolds Numbers of the full-size airship.

3. Origin of negative or stern-to-bow longitudinal force on airship model at 90° yaw.

4. Comparison of the drag results on the *Akron* model above the ground board in the full-scale tunnel with those measured in the 20-foot tunnel in free-air conditions.

5. Reason for the reversal of the pitching-moment coefficients of the model in the yaw-angle range between 30° and 60°.

6. The large yawing moments encountered at 150° yaw in contrast to the relative ineffectiveness of the vertical tail surfaces at angles of yaw between 0° and 60°.

**Origin of lift on airship.**—In the analysis of the flow and the aerodynamic forces on the airship the model has been considered as divided into sections of unit length of simple geometric form about which the flow may be predicted. Thus at small angles of yaw, sections through the airship parallel to the relative wind have profiles similar to thick symmetrical airfoils; whereas at larger angles of yaw, these sections parallel to the wind are deformed into approximately elliptical shapes that become circles at 90°. The flows over both the symmetrical airfoil sections and the bluff elliptical and circular sections are well known and have been the subject of many previous investigations. It has been shown that to obtain a lift from these sections, i. e., the airfoil or circular sections, it is required that a circulation exist, the circulation manifesting itself by different velocities and pressures over the bottoms and tops of the profiles.

The existence of a lift on the airship model therefore indicates a circulation about the sections and, inasmuch as the angle of attack of the profiles is 0°, the entire circulation may be attributed to the interference of the ground board and ground gradient. This same conclusion is obvious from the symmetry of the model and, in the absence of a ground plane and velocity gradient, no lift would be expected on the model.

It is believed that the resultant circulation producing a vertical force may be contributed from the three following sources:

1. Contraction of flow between model and ground board.
2. Unsymmetrical flow in the wake of the model due to the ground-board restraint.
3. Unsymmetrical pressure distribution over top and bottom of model due to the velocity gradient.

The contraction of the flow between the airship and the ground board produces lower pressures on the bottom side of the model with a resultant downward or negative lift, which increases as the model approaches the ground. The magnitude of this effect may be theoretically computed (reference 7) assuming potential flow over the model and no ground gradient. For this calculation the ground plane is replaced by a

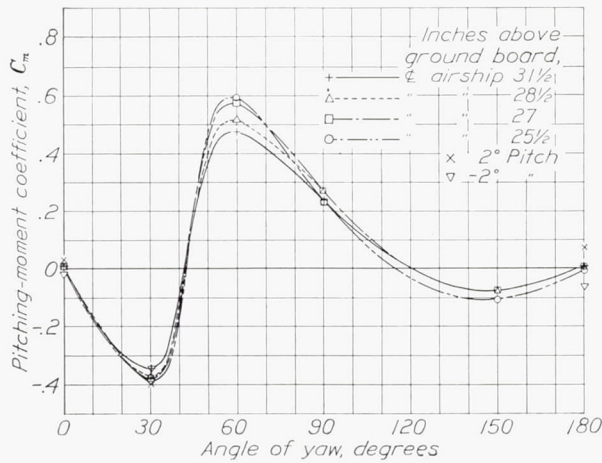


FIGURE 16.—The variation of pitching-moment coefficient with angle of yaw, angle of pitch, and height above the ground board at a Reynolds Number of 16,000,000.

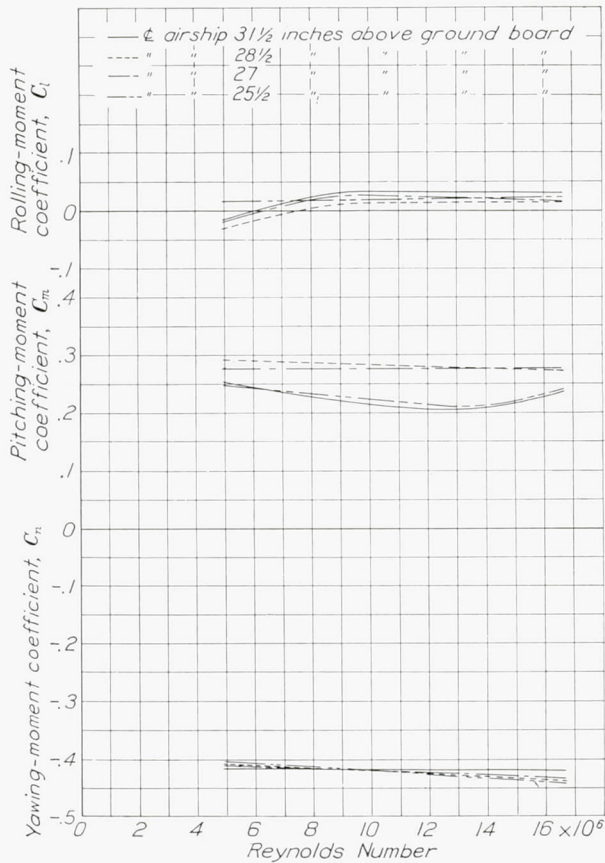


FIGURE 18.—The variation of yawing-moment coefficient, pitching-moment coefficient, and rolling-moment coefficient with Reynolds Number. Model at 90° yaw.

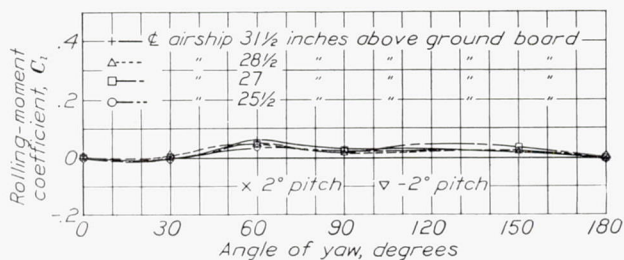


FIGURE 21.—The variation of rolling-moment coefficient with angle of yaw, angle of pitch, and height above the ground board at a Reynolds Number of 16,000,000.

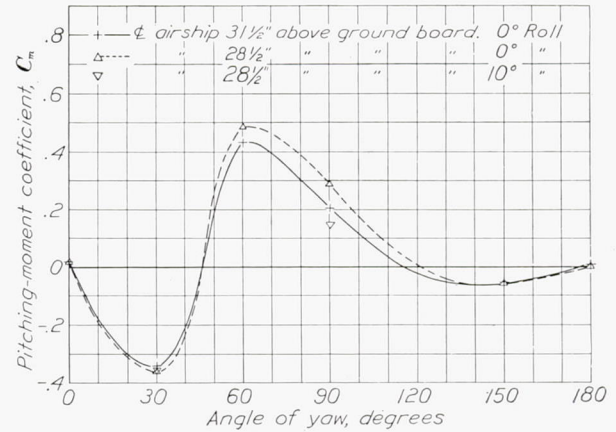


FIGURE 17.—The variation of pitching-moment coefficient with angle of yaw, angle of roll, and height above the ground board at a Reynolds Number of 8,000,000.

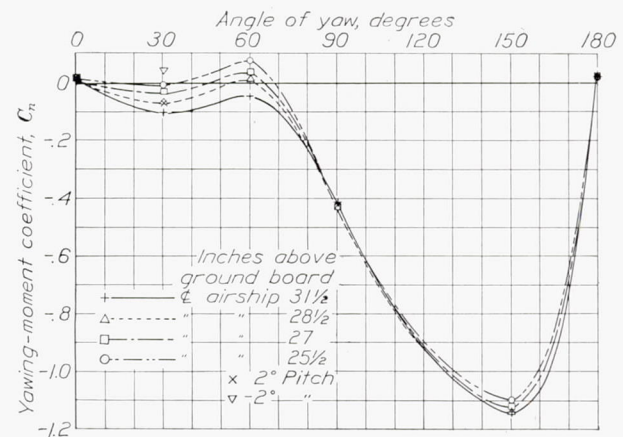


FIGURE 19.—The variation of yawing-moment coefficient with angle of yaw, angle of pitch, and height above the ground board at a Reynolds Number of 16,000,000.

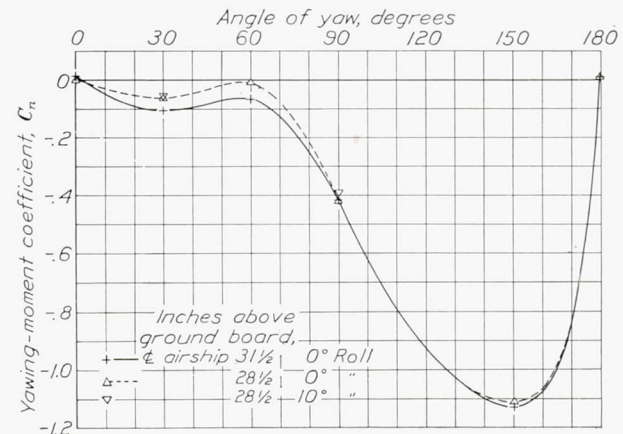


FIGURE 20.—The variation of yawing-moment coefficient with angle of yaw, angle of roll, and height above the ground board at a Reynolds Number of 8,000,000.

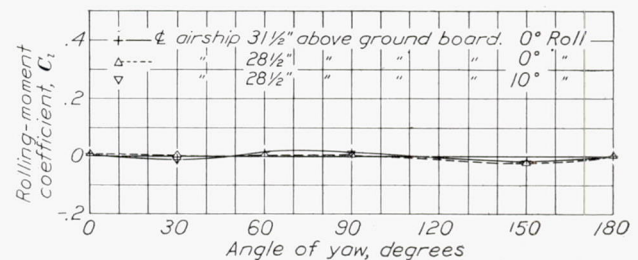


FIGURE 22.—The variation of rolling-moment coefficient with angle of yaw, angle of roll, and height above the ground board at a Reynolds Number of 8,000,000.

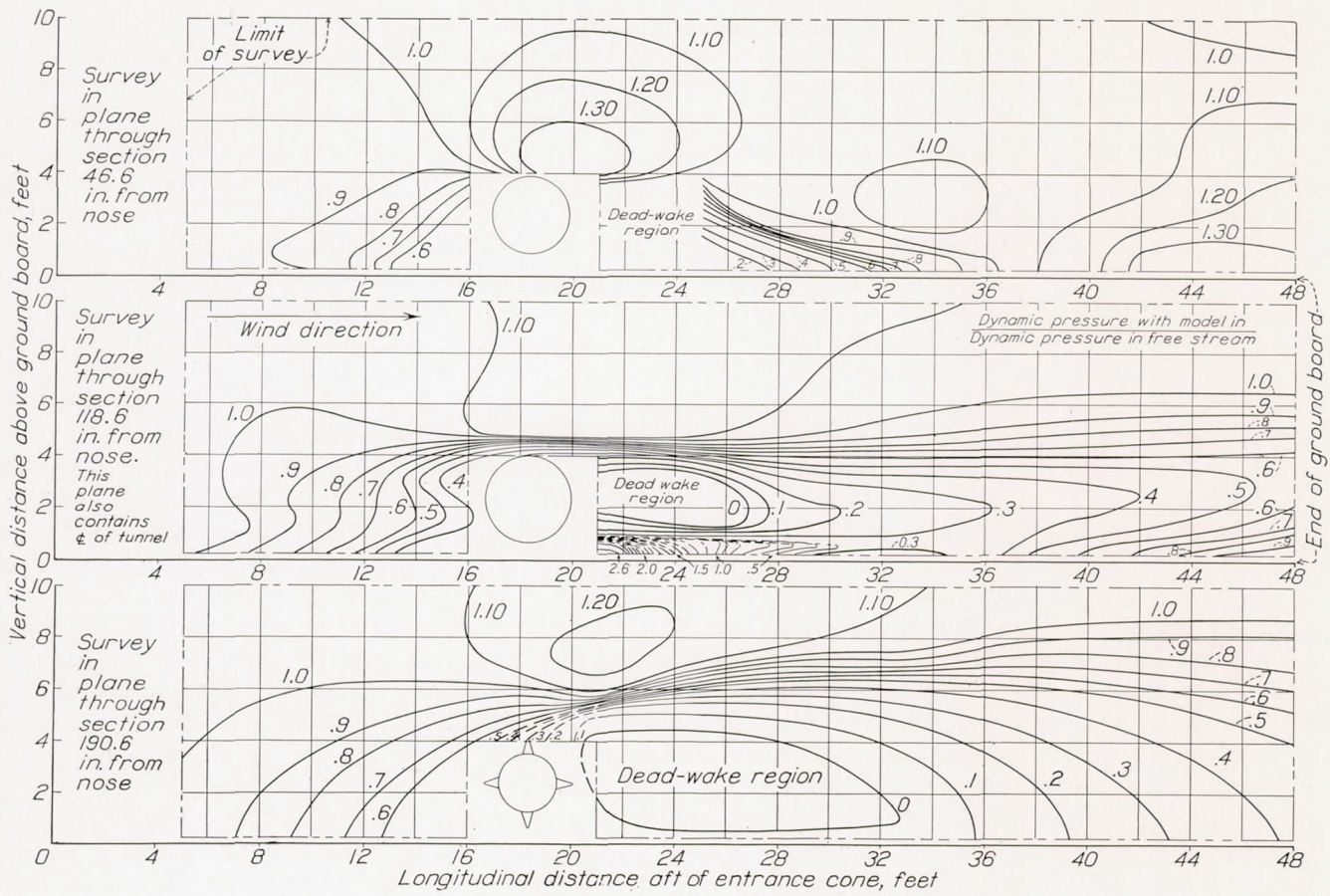


FIGURE 23.—Survey of dynamic pressure in the wake of the airship model at 90° yaw.

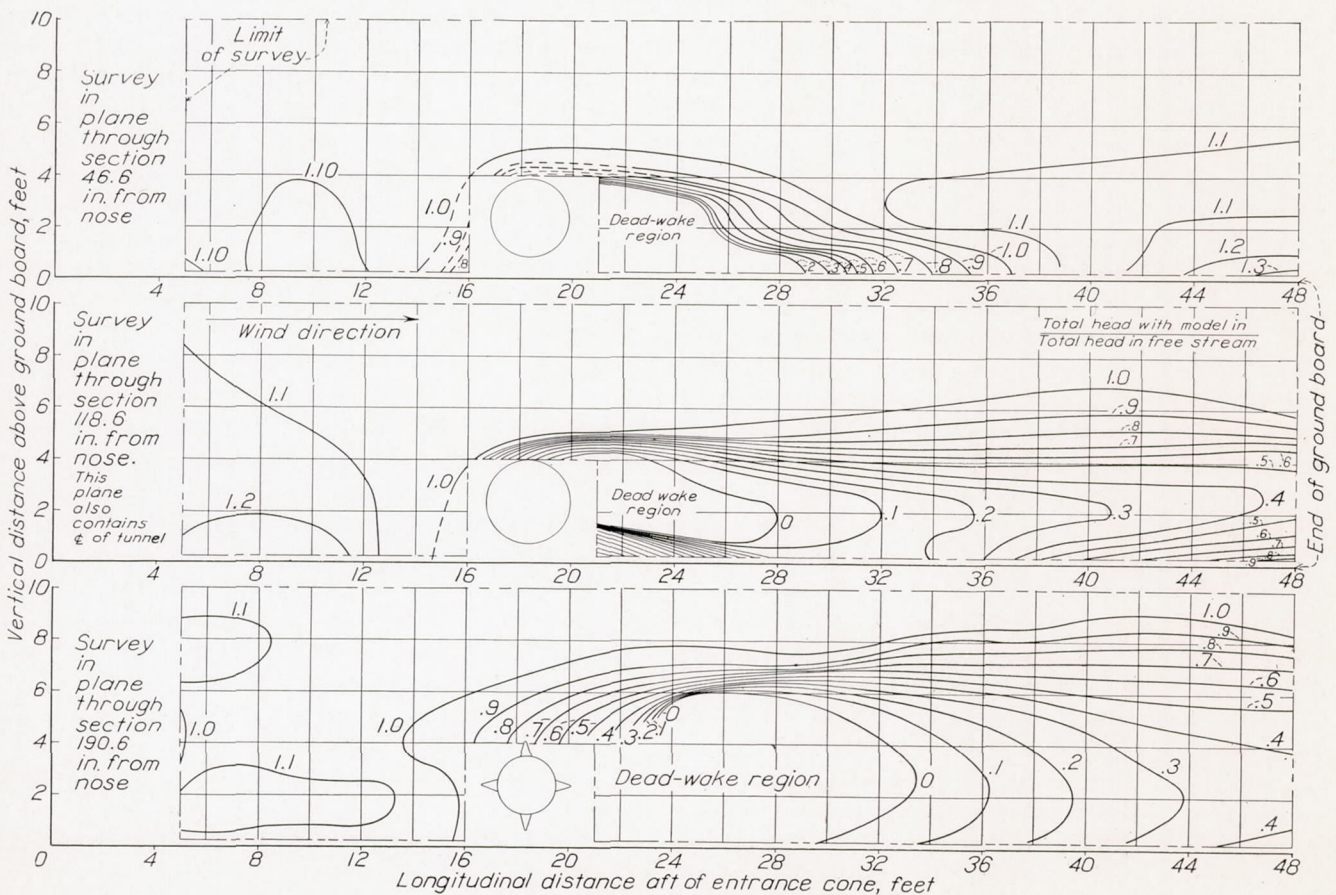


FIGURE 24.—Survey of the total pressure in the wake of the airship model at 90° yaw

reflected image of the model in the ground plane. Computations of this type made for the condition of the airship at  $90^\circ$  yaw indicate that, if the flow over the model were truly potential, the attraction of the model to the ground plane would be large and the resultant lift force negative rather than positive.

The assumption of potential flow over the model is wholly erroneous, in fact, it is only at angles of yaw near  $0^\circ$  that any similarity exists between the theoretical and the actual flow over the hull. This disparity with the theoretical condition is caused by the breakaway of the flow from the surface of the model over the rear of the sections owing to the losses in the boundary layer. The air flow will not follow the hull but separates forming a dead-air region of negative pressure behind the model. The size of the dead-air region is dependent on the shape of the sections over which the air passes, being smallest for the  $0^\circ$  yaw condition (fig. 4(a)) and largest for the  $90^\circ$  yaw angle. (See smoke pictures fig. 4(j) and 4(k) and the wake surveys behind the model at  $90^\circ$  yaw in figs. 23 and 24.) Approximate computations based on flows over the airship model including separation over the rear of the model revealed much smaller negative-lift effects arising from the contraction than were previously computed from the potential flow and indicate that the contraction effect may be one of the less important of the effects contributing to the resultant vertical force.

The second source of lift is similar to the first in that it is related to the effect of the ground plane on the flow. It particularly depends on the effect of the ground board on the flow over the leeward portions of the airship profiles and on the point of separation of the flow from the surface. Previous tests have shown the point of separation to be very sensitive to any type of interference effect, and several stable types of flow are possible, depending upon the particular set of external interference conditions. The effect of the unsymmetrical restraint is to rotate the flow in front of the model upward and to induce a positive angle of attack in the flow over the model. The flow over the bottom of the airship therefore tends to follow farther along the circumference of the model before separation than the flow over the top side, and the dead-wake region of negative pressure on the leeward side of the model is rotated upward, resulting in a positive lifting force. Indications of these effects are shown by the smoke pictures. The flow over the model at  $60^\circ$  yaw (maximum-lift angle) is shown in figure 4(g) and it may be observed that the dead-air region is shifted upward and that the flow follows much farther around the lower half of the model than over the upper half. This unsymmetrical pattern in the wake is also shown in figures 4(e) and 4(i). The upflow in front of the model for the  $30^\circ$  yaw condition is shown in figure 4(c), and for the  $90^\circ$  yaw condition in figures 4(i) and 4(k). The effect of the ground board on the breakaway appears

to be smallest for the  $90^\circ$  angle (figs. 4(j) and 4(k)) probably because of the shorter effective chord in the direction of the flow. This observation is also a check on the smaller positive force measured at this angle.

The third factor contributing to the vertical force is the ground gradient. Inasmuch as the pressures on the surface of the body are a function of the dynamic pressures outside the field of the body, the pressures over the surface at positions where the outside velocity is highest will reach larger values. In this particular case, therefore, with a positive gradient, that is, a velocity increasing with height above the ground board, the pressures on the upper side of the airship model will reach higher negative values than those on the lower surface and produce a positive lift. Trial computations were made assuming average velocities over the top and bottom half of the airship when at  $90^\circ$  yaw; integration of the computed pressures over the surface of the model gave a positive lift of the same sense but of slightly greater magnitude than the measured one. The method was, of course, approximate, inasmuch as the velocity varies continuously with the height, and it was also necessary to make assumptions as to the pressure distribution over the cylindrical profile. The results indicate, however, that the ground gradient is an important factor contributing to the lifting force.

The large effect of the velocity gradient on the lift force suggests that further tests be made with other velocity gradients than the one employed in the present investigation. Generally the results should indicate greater positive lifts with higher velocity gradients than that of the present investigation, and conversely.

All three factors to which the vertical force has been attributed—streamline contraction, unsymmetrical wake restraint, and ground gradient—vary with the height, and the measured lift force did show a slight change with the model height; in the range of the tests, however, there were no critical points at which either sudden changes or reversals of forces existed.

**Extrapolation of results.**—The results showing a positive lift on the model airship are of particular interest in regard to the possibility of predicting the lift of the full-size airship. The extrapolation of results from the model to the full-size airship is lengthy inasmuch as the Reynolds Numbers for the full-scale airship at wind velocities of 20 miles per hour are about eight times the maximum value for the tests in the full-scale tunnel. A direct extrapolation by continuation of the curves of model results to the Reynolds Numbers of the full-size airship is not believed justified or satisfactory, inasmuch as the extension of a curve to eight times its original length will, no doubt, lead to erroneous conclusions.

A more satisfactory method is to consider the flows about the body for the two cases of model and full scale to see if any critical changes in the flow are to be expected in passing through the scale range to be



extrapolated. It has been previously mentioned that at large angles of yaw longitudinal sections of the airship become elliptical and, at  $90^\circ$ , become circular. Two stable types of flow over a cylinder at right angles to the flow may occur, depending upon the Reynolds Number. For Reynolds Numbers below the critical (400,000 to 500,000 based on cylinder diameter) the flow is characterized by an early separation on the rear of the cylinder, the breakaway occurring slightly before the point of maximum width (fig. 25(a)). For Reynolds Numbers above the critical the boundary layer becomes turbulent and the breakaway occurs farther back along the circumference (fig. 25(b)). Quite marked differences would therefore be expected in the flow over the airship and in the forces on the model in passing through this Reynolds Number range. In the present model tests the Reynolds Number was above the critical for all but a few of the smallest sections near the bow and stern of the model.

Tests have been made in other wind tunnels of cylinders adjacent to ground boards (references 1 and 2) but, owing to the fact that all of the results were obtained close to the critical Reynolds Numbers, they show different results from the full-scale-tunnel data. Once the critical range has been passed, the flow in cylinder tests has shown no marked changes with the Reynolds Number, and it is believed that the flow over the full-size airship will be generally similar to that over the model as tested in the full-scale tunnel. It may be further pointed out that the portion of the lift caused by the ground gradient should scale almost directly to the larger Reynolds Numbers. It is believed that the lift curve (fig. 8), which show a decreasing lift with increasing Reynolds Number, will tend to flatten out at the very high Reynolds Numbers and show a more nearly constant value.

If the measured lift coefficients on the model airship at the highest Reynolds Numbers tested in the tunnel are scaled directly to the case of the full-size airship, the resultant vertical forces are of large magnitude for appreciable angles of yaw and moderate wind velocities. For example, the lift on an airship of the size of the *Akron* at  $30^\circ$  yaw in a 20-mile-per-hour wind velocity when its center line is about 95 feet above the ground is 17,800 pounds; for a yaw angle of  $60^\circ$  and the same wind velocity, the lift would reach a maximum of about 25,600 pounds. The Reynolds Number of this typical case is about eight times the highest value reached in the tunnel tests. The 95-foot height in full scale corresponds to the  $28\frac{1}{2}$  inch test height with the model.

**Longitudinal force.**—The large negative longitudinal force (with reference to body axis) at  $90^\circ$  yaw is of interest and may be accounted for by the unsymmetrical flow over the bow and stern of the airship. The flow over the bow produces a negative pressure region

over almost its entire area, whereas the flow over the stern is distributed by the tail surfaces and the static pressure is positive on the windward side and negative on the leeward (figs. 4(k) and 4(i)). The result is a longitudinal force in the direction of the nose. On the bare hull without tail surfaces the large negative value would not be expected.

**Comparison with drags measured in 20-foot tunnel.**—The model tested in the full-scale tunnel adjacent to the ground board had previously been tested in the N. A. C. A. 20-foot tunnel in the center of the free stream (reference 4). The minimum drag coefficient of 0.024 obtained from these tests may be compared with the  $0^\circ$  yaw value from the full-scale-tunnel tests. The

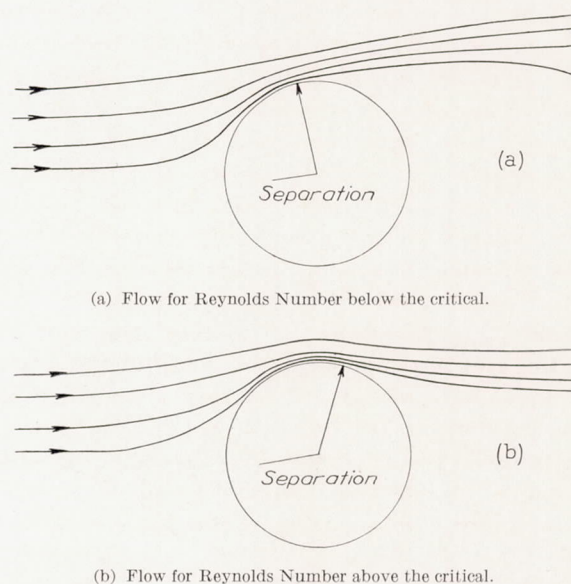


FIGURE 25.—Flow over circular cylinders showing separation.

comparison indicates the magnitude of interference effect on the drag owing to the ground board and the ground gradient. In the comparison, consideration must be given to the fact that coefficients for the full-scale-tunnel tests were not based on the average velocity over the model but on the velocity at 5 feet above the board. If the true average dynamic pressure over the model is used, the drag coefficient for the full-scale-tunnel tests at  $0^\circ$  yaw becomes 0.039, indicating that the interference increased the drag approximately 60 percent above the 20-foot-tunnel value. Approximate computations for the  $90^\circ$  angle of yaw, considering the airship to consist of a series of cylinders and the tail surfaces to be flat plates, gave a free-air drag coefficient of 1.27. This value was compared with the measured drag coefficient at  $90^\circ$  yaw corrected to the actual dynamic pressure over the model, and the interference of the ground plane and gradient on the drag was again shown to be in the order of 60 to 70 percent. The increase in drag may be attributed largely to the disturbed wake of the model.

**Reversal of pitching moment.**—The reversal of the sign of the pitching moments in the yaw-angle range between  $30^\circ$  and  $60^\circ$  is probably caused by the changing force on the horizontal tail surfaces. The large negative moment at  $30^\circ$  is caused by a large positive lift on the horizontal tail surfaces, inasmuch as the smoke pictures in figure 4(e) show the average flow in the tail vicinity to be inclined upward. At the  $30^\circ$  angle the flow over the windward horizontal surface is not yet shielded by the vertical surfaces, the blanketing action being counteracted by the tendency of the flow to follow along the hull and reduce the effective angle of yaw. Figures 4(c) and 4(e) show this effect clearly. At the  $60^\circ$  angle, however, the vertical surfaces effectively shield the flow over the entire horizontal surfaces and the areas become inactive (fig. 4(h)). The hull pressures are, moreover, in the correct direction to create a positive moment, as is observed in figure 4(f), which indicates that the flow between the airship and the ground plane is toward the stern. In all probability there is a low-pressure region under the stern and a down force at the tail. For the  $30^\circ$  angle it may be observed that the smoke streamers passing between the board and the airship are turned toward the bow.

**Effect of yaw angle on yawing moment.**—The measured yawing moments were small in the range of yaw angles between  $0^\circ$  and  $60^\circ$  but changed to large negative values at  $150^\circ$  (figs. 19 and 20).

The small yawing moments in the yaw-angle range between  $0^\circ$  and  $60^\circ$  are explained somewhat by the smoke picture 4(e), which shows that the air is turned by the hull and flows along the hull in the region of the tail. The effective angle of attack of the fin, and therefore the fin lift, is thus reduced. For the  $150^\circ$  yaw angle, however, the fin is ahead of the hull and operates in an air stream free of interference. The effectiveness of the fin when forward of the hull is shown in figure 4(i) where the large bending of the smoke streamers owing to the downwash from the fin is readily apparent. These results verify previous experimental information showing the effectiveness of bow elevators.

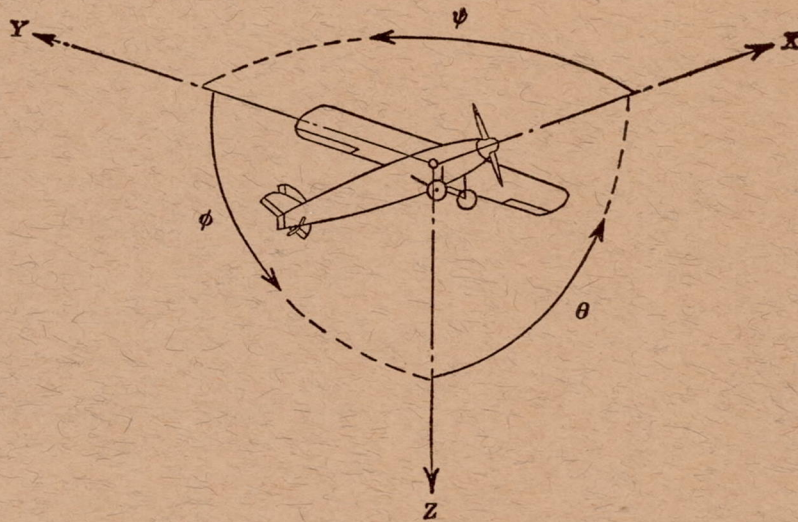
## CONCLUSIONS

1. Changes in the angle of yaw of the airship greatly affect the ground-handling forces; whereas, in the range of Reynolds Numbers between 5,000,000 and 19,000,000 (Reynolds Numbers based on model length), small changes in height, pitch, or roll of the airship have a negligible effect.
2. In the scale range investigated the ground-handling forces are not importantly affected by changes in Reynolds Numbers.
3. The curves of the model results should not be extrapolated to the Reynolds Numbers of the full-size airship but may be used with some reliability directly from the measured values at the highest Reynolds Numbers.
4. The application of the measured results to the full-size airship shows very large handling forces for appreciable angles of yaw and moderate wind velocities.

LANGLEY MEMORIAL AERONAUTICAL LABORATORY,  
NATIONAL ADVISORY COMMITTEE FOR AERONAUTICS,  
LANGLEY FIELD, VA., *April 8, 1936.*

## REFERENCES

1. Knoblock, F. D., and Troller, Th.: Tests on the Effect of Sidewind on the Ground Handling of Airships. Daniel Guggenheim Airship Inst., Publication No. 2, 1935, pp. 53-57.
2. Bradfield, F. B., and Cohen, J.: Wind Tunnel Test of Lift and Drag Measured in a Velocity Gradient. R. & M. No. 1489, British A. R. C., 1932.
3. DeFrance, Smith J.: The N. A. C. A. Full-Scale Wind Tunnel. T. R. No. 459, N. A. C. A., 1933.
4. Freeman, Hugh B.: Force Measurements on a 1/40-Scale Model of the U. S. Airship "Akron." T. R. No. 432, N. A. C. A., 1932.
5. Thompson, F. L., Peck, W. C., and Beard, A. P.: Air Conditions Close to the Ground and the Effect on Airplane Landings. T. R. No. 489, N. A. C. A., 1934.
6. Theodorsen, Theodore, and Silverstein, Abe: Experimental Verification of the Theory of Wind-Tunnel Boundary Interference. T. R. No. 478, N. A. C. A., 1934.
7. Garrick, I. E.: Potential Flow about Arbitrary Biplane Wing Sections. T. R. No. 542, N. A. C. A., 1936.



Positive directions of axes and angles (forces and moments) are shown by arrows

Axis		Force (parallel to axis) symbol	Moment about axis			Angle		Velocities	
Designation	Sym- bol		Designation	Sym- bol	Positive direction	Designa- tion	Sym- bol	Linear (compo- nent along axis)	Angular
Longitudinal	X	X	Rolling	L	Y → Z	Roll	$\phi$	u	p
Lateral	Y	Y	Pitching	M	Z → X	Pitch	$\theta$	v	q
Normal	Z	Z	Yawing	N	X → Y	Yaw	$\psi$	w	r

Absolute coefficients of moment

$$C_l = \frac{L}{qbS}$$

(rolling)

$$C_m = \frac{M}{qcS}$$

(pitching)

$$C_n = \frac{N}{qbS}$$

(yawing)

Angle of set of control surface (relative to neutral position),  $\delta$ . (Indicate surface by proper subscript.)

#### 4. PROPELLER SYMBOLS

$D$ , Diameter

$p$ , Geometric pitch

$p/D$ , Pitch ratio

$V$ , Inflow velocity

$V_s$ , Slipstream velocity

$T$ , Thrust, absolute coefficient  $C_T = \frac{T}{\rho n^2 D^4}$

$Q$ , Torque, absolute coefficient  $C_Q = \frac{Q}{\rho n^2 D^5}$

$P$ , Power, absolute coefficient  $C_P = \frac{P}{\rho n^3 D^5}$

$C_s$ , Speed-power coefficient =  $\sqrt[5]{\frac{\rho V^5}{P n^2}}$

$\eta$ , Efficiency

$n$ , Revolutions per second, r.p.s.

$\Phi$ , Effective helix angle =  $\tan^{-1} \left( \frac{V}{2\pi r n} \right)$

#### 5. NUMERICAL RELATIONS

1 hp. = 76.04 kg-m/s = 550 ft.-lb./sec.

1 metric horsepower = 1.0132 hp.

1 m.p.h. = 0.4470 m.p.s.

1 m.p.s. = 2.2369 m.p.h

1 lb. = 0.4536 kg.

1 kg = 2.2046 lb.

1 mi. = 1,609.35 m = 5,280 ft.

1 m = 3.2808 ft.